Influence of Bis Thiourea Nickel Nitrate on structural, optical, electrical, thermal and mechanical behavior of KDP single crystal for NLO applications

Influence of Bis Thiourea Nickel Nitrate on structural, optical, electrical, thermal and mechanical behavior of KDP single crystal for NLO applications

Y. B. Rasal[a], R. N. Shaikh[a], M. D. Shirsat[b], S. Kalainathan[c], S. S. Hussaini[a*]

[a]Crystal Growth Laboratory, Department of Physics, Milliya Arts, Science and Management Science College, Beed-431122, Maharashtra, India

[b]Intelligent Materials Research Laboratory, Department of Physics, Dr. Babasaheb Ambedkar Marathwada University, Aurangabad-431005, Maharashtra, India

[c]Centre for Crystal Growth, School of Advanced sciences, VIT University, Vellore - 632014, India

Abstract

A Single crystal of bis-thiourea nickel nitrate (BTNN) doped potassium dihydrogen phosphate (KDP) has been grown from solution at room temperature by slow evaporation technique. The cell parameters of the grown crystals were determined using single crystal X-ray diffraction analysis. The different functional groups of the grown crystal were confirmed using Fourier transform infrared analysis. The improved optical parameters of grown crystal have been evaluated in the range of 200-900 nm using the UV-visible spectral analysis. The grown crystal was transparent in the entire visible region and Band gap value is found to be 4.96 eV. The influence of bis-thiourea nickel nitrate on third order nonlinear optical properties of KDP crystal has been investigated by means of Z-scan technique. The Second harmonic generation (SHG) efficiency of grown crystal measured using Nd-YAG laser is 1.98 times higher than that of pure KDP. The third order nonlinear optical susceptibility (χ_3) and nonlinear absorption coefficient (β) of BTNN doped KDP crystal is found to be 1.77 x 10^{-5} esu and 5.57 x 10^{-6} cm/W respectively. The laser damage threshold (LDT) energy for the grown crystal has been measured by using a Q-switched Nd:YAG laser source. The bis-thiourea nickel nitrate shows authoritative impact on dielectric properties of doped crystal. The influence of bis-thiourea nickel nitrate on the mechanical behavior of KDP crystal has been investigated using Vickers microhardness intender. The thermal behavior of BTNN doped KDP crystal has been analyzed by TGA/DTA analysis.

Keywords: Crystal growth, Nonlinear optical materials, Mechanical studies, Dielectric studies, Thermal studies.

1. Introduction

In various interdisciplinary frontier fields nonlinear optical (NLO) single crystals play very crucial role in designing/tuning/processing/fabricating the technologically essential devices readily used in photonics, optoelectronics, laser frequency conversion and integrated optic applications [1-2]. The potassium dihydrogen phosphate (KDP) crystal shows high technological impetus for industrial applications owing to high NLO response and excellent optical homogeneity which are various experimental approaches (doping of additives or different growth techniques) have been attempted, however, the stress prerequisite on parameters for designing optical switching device. For the enhancement in desired qualities of KDP crystal has been given on doping technique. In literature, majority investigations were reported on enhancing the effect of amino acids (glycine, L-alanine, L-

Corresponding author: email id: shuakionline@yahoo.co.in, Mob. No. +91-9325710500

arginine, L-histidine, L-valine) on the nonlinear optical property of KDP crystal [3-5]. The influence of formic acid, maleic acid and oxalic acid on SHG efficiency, third order nonlinear optical and dielectric properties of KDP crystal have been extensively studied [6-8]. In addition, the impact of metallic impurities (Al^{3+}, Na^{+}) and different dyes on optical, mechanical, thermal and dielectric traits of KDP crystal has also been investigated [9-11]. In our recent investigation, the doping of bis-thiourea zinc chloride (BTZC) has inculcated enhancement in SHG efficiency, optical transparency and crystalline quality of KDP crystal, dielectric quality [12].

In literature, there is the least work on thiourea metal complex mixed KDP crystals; P. Kumaresan et al have reported the effect of copper thiourea complex on KDP in view of structural, optical transmittance and thermal behavior [13]. Hence in the present investigation; the attention is focused on the influence of thiourea metal complex Nickel thiourea nitrate (BTNN) on KDP. The grown crystals were subjected to structural, optical, electrical, thermal and mechanical properties of KDP for its improved NLO applications. The third-order non-linear properties of the grown crystal have been discussed in detail by using the Z-Scan technique.

2. Experimental procedure

The BTNN salt was synthesized using analytical grade thiourea and nickel nitrate taken in the ratio (2:1) and dissolved in analytical reagent ethanol and deionized water in the equal ratio as reported in the literature [14]. The supersaturated solution of KDP salt was prepared at room temperature by gradually dissolving the AR grade KDP salt (99%). The 0.1 and 0.2 mole % of BTNN is added with constant stirring in the supersaturated solution of KDP in separate beakers. The prepared solutions were allowed to evaporate at room temperature to procure the respective salts. In the Kurtz–Perry powder test 0.2 mole% of BTNN doped KDP crystal has higher second order nonlinear response. Hence the saturated solution of 0.2 mole% of BTNN doped KDP was prepared and allowed to evaporate at a temperature of 35^{o}C. The optical quality 0.2 BTNN doped KDP (BTNN+KDP) single crystal of size 42×14×7 mm^3 grown within two weeks is shown in figure 1.

3. Results and discussion

3.1 Single crystal x-ray diffraction studies

The single crystal x-ray diffraction studies of 0.2 mol %BTNN doped KDP crystal was carried out using Enraf Nonius CAD4-MV31 crystal X-ray diffractometer. From the single crystal XRD analysis, it is confirmed that the crystal belong to the tetragonal I crystal system with chiral space group I (-4)2d (space group number = 122) and the determined lattice parameter values are a = b = 7.49Å, c = 7.00Å and $\alpha = 90^0$, $\beta = 90^0$, $\gamma = 90^0$ with volume =393 $(Å)^3$. The lattice parameter values of pure KDP are a = b =7.44 Å, c = 6.94Å and with volume 384$(Å)^3$. Thus the dopant Bis Thiourea Nickel Nitrate insists the lattice strain on KDP crystal introduced by slight change in unit cell parameters of doped KDP [12].

3.2 Fourier transform infrared (FT-IR) analysis

The grown crystals were subjected to FTIR analysis to analyze the presence of functional groups quantitatively. The spectrum was recorded using Bruker α-ATP spectrophotometer in the range of 550-4000 for BTNN doped KDP crystals are shown in figure 2. The observed vibrational frequencies and their assignments for pure and doped KDP are listed in Table 1. The broad absorption bands 2750-3700 cm^{-1} were assigned to stretching of NH_2 frequencies in

pure KDP and doped KDP crystals. The absorption bands 2667 cm^{-1}, 1456 cm^{-1} are assigned to C-H stretching. The band assigned at 2345 cm^{-1} correspondence to O-H stretch. In the doped KDP spectrum, absorption peak 2167 cm^{-1} observed belongs to O-H, N-H stretching is observed at peaks 2030 cm^{-1}, 638 cm^{-1} respectively and 722 cm^{-1} peaks were assigned to N-H waging. Similarly, the same peaks in pure KDP are slightly differed by frequencies and observed at 2223 cm^{-1}, 2055 cm^{-1},620 cm^{-1} and 743 cm^{-1} for O-H, N-H stretching and N-H waging respectively [10]. The O=P–OH stretching absorption peak observed at 1597 cm^{-1} in doped KDP and 1596 cm^{-1} in pure KDP [15]. The additional peaks observed at 820 cm^{-1} and 1393 cm^{-1} in the absorption spectra belongs to $Ni_3(PO_4)_2$ and KNO_3 respectively [16]. The P=O stretching peak finds at 1080 cm^{-1} and C-O stretching at 952 cm^{-1}. The present FT-IR study on pure and doped KDP clearly indicates the effect of BTNN dopant on the crystal structure of pure KDP.

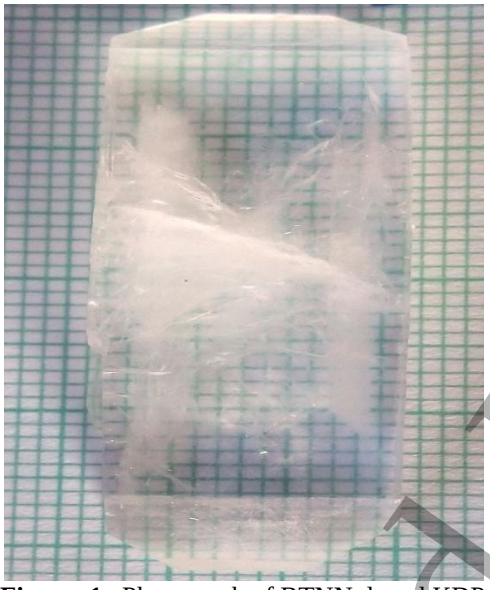

Figure 1 Photograph of BTNN doped KDP crystal

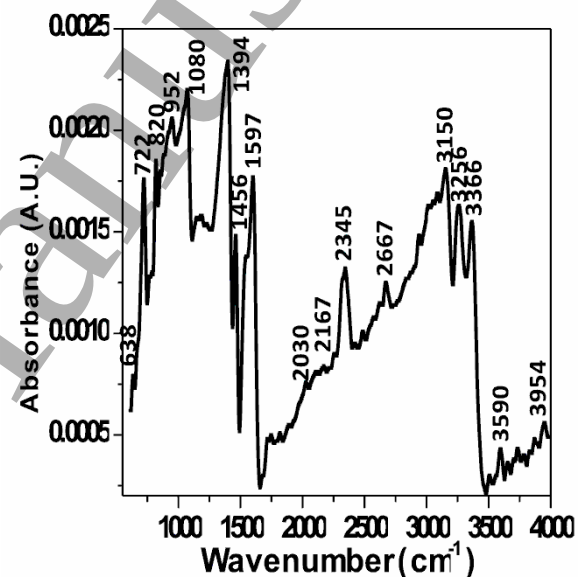

Figure 2 FT-IR of doped crystal

Table 1 Observed IR frequencies (cm^{-1}) of pure KDP and BTNN doped KDP

Pure KDP	Doped KDP	Assignment
3245	3256	P–O–H bending of KDP
	2667	CH stretching
2374	2345	O-H stretching
2223	2167	O-H,N-H stretching
	2030	N-H stretch
1596	1597	O=P–OH stretching
1434	1456	C-H stretching
	1394	KNO_3
1091	1080	P=O stretching
	952	C-O stretching
	820	$Ni_3(PO_4)_2$
	722,638	N–H wagging, N-H stretching
2750-3700	2750-3700	Symmetric and asymmetric stretching of O-H, NH_2

3.3 Optical Properties

3.3.1 SHG efficiency test

The Kurtz-Perry powder SHG test has been carried out using the Q-switched Nd:YAG laser [17]. The output of laser source with Pulse energy 5.4 μJ/pulse, and pulse of width 6 ns with a repetition rate of 10 Hz was used. The finely grinded uniform samples of KDP and BTNN doped KDP was exposed by a beam of Nd:YAG laser having wavelength 1064 nm. Second Harmonic radiation generated by the randomly oriented microgrants was focused by a lens and detected by a photomultiplier tube. The emission of sharp green light from the crystalline powder confirmed the second order NLO behavior of BTNN doped KDP [18]. The Figure 3 is the plot of SHG output intensity (CPS) vs. the wavelength and shows the output intensities of pure and doped KDP crystal. The SHG efficiency of 0.1 and 0.2 mol% BTNN doped KDP crystal was found to be 1.65 and 1.98 times that of potassium dihydrogen phosphate (KDP) respectively. The Table 2 shows comparisons of SHG efficiency of doped KDP crystal. The SHG efficiency increased with the increase in doping % of BTNN. Thus grown crystal may be efficient NLO material for applications in laser frequency conversion and nonlinear applications [19].

Table 2 SHG analysis data

Crystal sample	SHG efficiency	Reference no.
KDP	1.0	Present study
1 mol% OA + KDP	1.41	8
1 mol% MA + KDP	1.82	8
1 mol% + Formic acid	1.13	12
0.2 mol% BTZC + KDP	1.65	12
0.1mol% BTNN + KDP	1.65	Present study
0.2 mol% BTNN + KDP	1.98	Present study

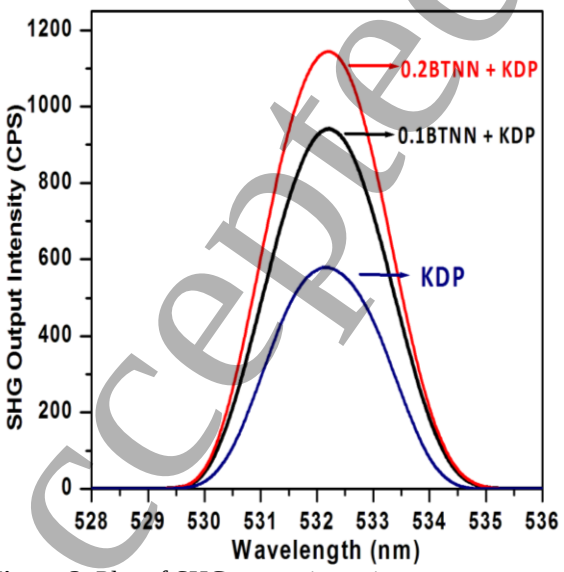

Figure 3 Plot of SHG output intensity

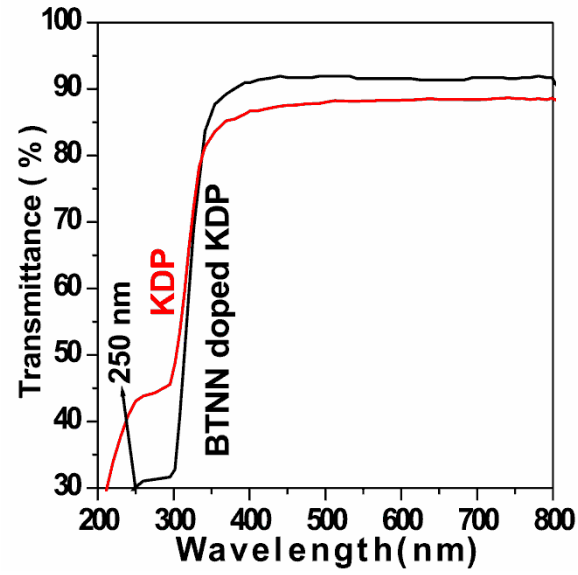

Figure 4 Transmittance spectrum

3.3.2 UV–visible studies

The optical transmission spectra of the grown crystals of thickness 2 mm were recorded using Shimadzu UV-2450 spectrophotometer in the range 200-900 nm is shown in figure 4. The BTNN doped KDP crystal showed high transparency in the entire visible region of 92% and lower cut-off wavelength of 250 nm suggests its suitability for NLO devices [20]. The optical band gap of the grown crystal was determined by using formula $E_g = 1240/\lambda$ where λ is the lower cut off wavelength (250 nm) determined by transmittance spectrum and is found to be 4.96 eV [20]. The optical absorption coefficient (α) is determined using the equation $\alpha = [2.303 \log (1/T)]/t$. The propagation of light through crystal medium as refractive index is determined by using formula $n = [1/T + (1/T - 1)]$ where T is Transmittance. The value of Refractive index of the doped material is found to be 1.45 at 632 nm. The reflectance is calculated in terms of the refractive index as by using formula $R = (n-1)^2/ (n+1)^2$ The plots refractive index and reflectance vs. wavelength is as shown in figure 5(a) and (b) respectively. From observations by graphs, it is concluded that the high transmittance, lower values of refractive index and reflectance in the entire visible region of a grown crystal having advantageous in applications of antireflection coating in solar thermal devices [21]. The optical conductivity as a function of photon energy was depicted in figure 6(a) and was calculated by using formula, $\sigma_{op} = \alpha nc/4\pi$,where c is the velocity of light. The positive response of optical conductivity with photon energy shows grown crystal have applications in information optical processing and computing [22]. The graph of the extinction coefficient of 0.2 mole% BTNN in response to photon to energy is depicted in figure 6(b), which concludes grown crystal, has lower values than KDP. The extinction coefficient was evaluated using the relation, $K= \lambda\alpha/2\pi$. The variation of extinction coefficient (K) helps to evaluate the loss of electromagnetic energy in visible region due to scattering and absorption phenomenon within the material medium. The value of real and imaginary susceptibilities has been calculated using the fundamental equations [21].

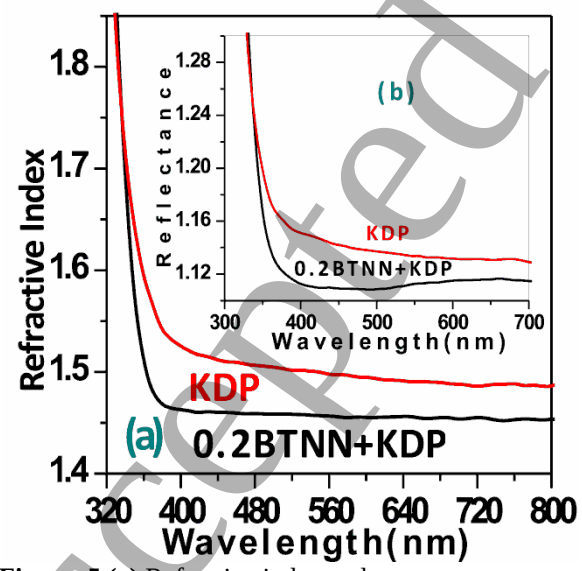

Figure 5 (a) Refractive index and **(b)** Reflectance vs. wavelength.

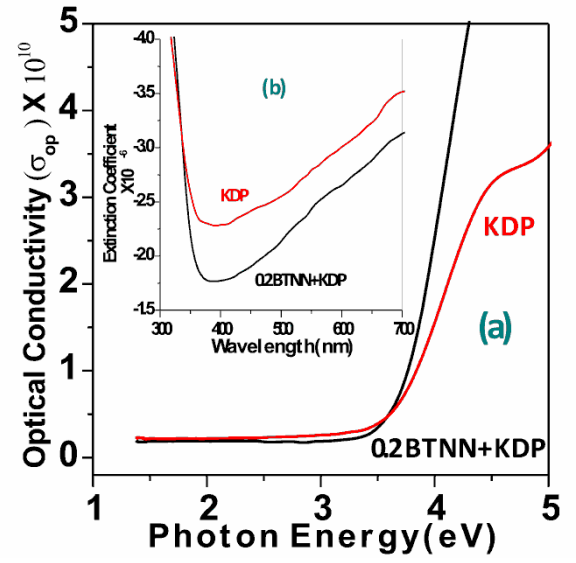

Figure 6 (a) Optical conductivity vs. E and **(b)** Extinction coefficient vs. wavelength.

The response of imaginary and real susceptibilities with photon energy are depicted in figure 7(a) and (b), it reveals that the real and imaginary dielectrics show lower values than pure KDP. The lower value of extinction coefficient

(10^{-6}), the high value of optical conductivity ($10^{10}S^{-1}$) and optical dielectric constant (real- 2.1 and imaginary - $4x10^{-2}$) of grown crystal is better for frequency conversion photonic devices [22]. The potential optical properties of the grown crystal suggest its suitability for UV tunable laser, NLO and SHG device applications effectively [23].

3.3.3 Z-scan studies

The single laser beam Z- scan integrated technique is discovered by Sheikh-Bahae et al. for to determine the third order nonlinear behavior of the material [24]. In this technique the closed aperture and open aperture data is measured simultaneously for to determine the third order nonlinear refractive index (n_2), susceptibility (χ) of the material and absorption coefficient (β).

In the present study the third-order NLO properties of well-polished 0.2 BTNN doped KDP crystal of size 0.5 mm is carried out using the Z-scan experimental technique (Table 3). The Gaussian beam of He-Ne laser of wavelength 632.8 nm is focused on crystal through the focal lens of focal length 30 cm. The crystal is varied from -Z to +Z direction that is along the path of the laser beam and the intensity of the beam is measured at a far distance. In closed aperture Z-scan configuration the position of crystal sample was changed along the Z direction and the transmittance was recorded through the closed slit of photodetector placed at a far distance. The aperture size and size of the crystal affects the transmitted intensity of the laser beam. The nonlinear refractive nature of crystal causes a self-focusing or self-defocusing effect.

The difference between the peak and valley transmission (ΔT_{p-v}) is given by equation as,

$$\Delta T_{p-v} = 0.406(1-S)^{0.25}\left|\Delta\phi\right| \quad (1)$$

Where, S= [1-exp ($-2r_a^2/\omega_a^2$)] is the aperture linear transmittance, r_a is the aperture radius and ω_a is the beam radius at the aperture.

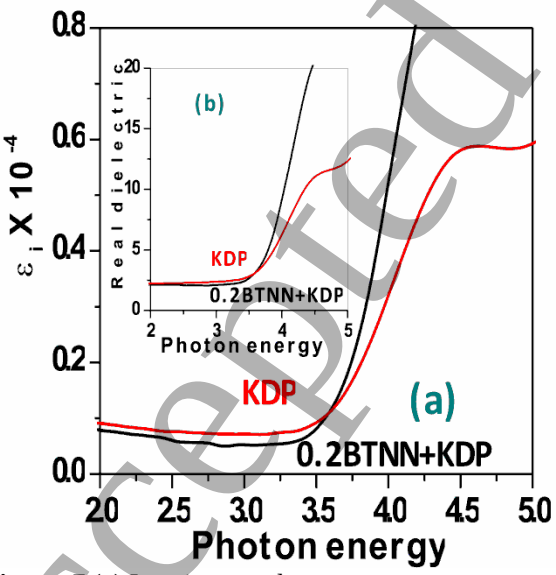

Figure 7 (a) Imaginary and **(b)** Real dielectric constant vs. E

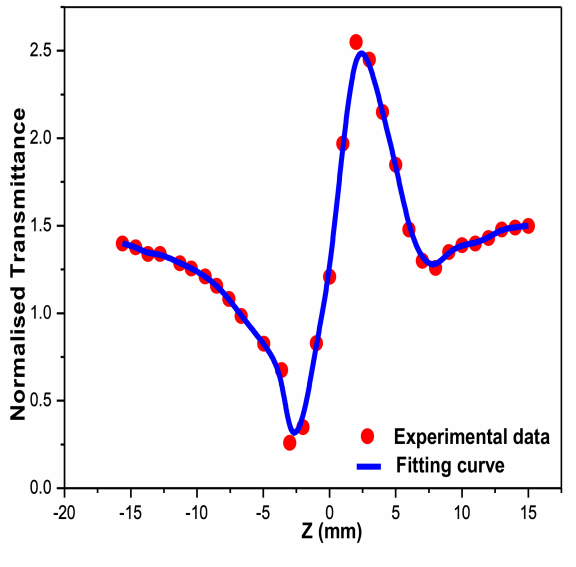

Figure 8 Close aperture curve

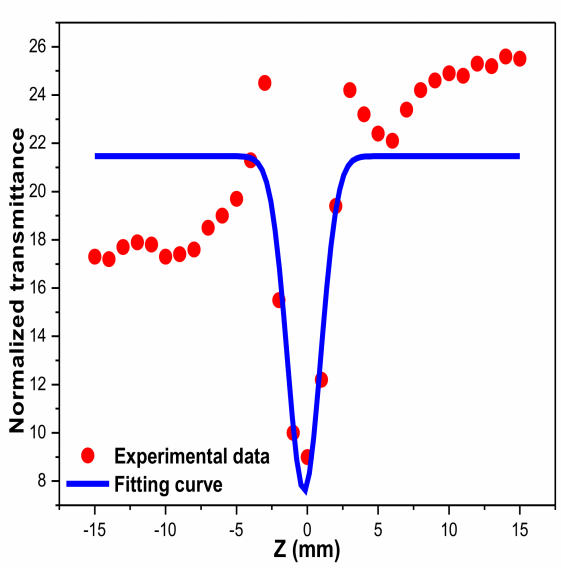

Figure 9 Open aperture curve

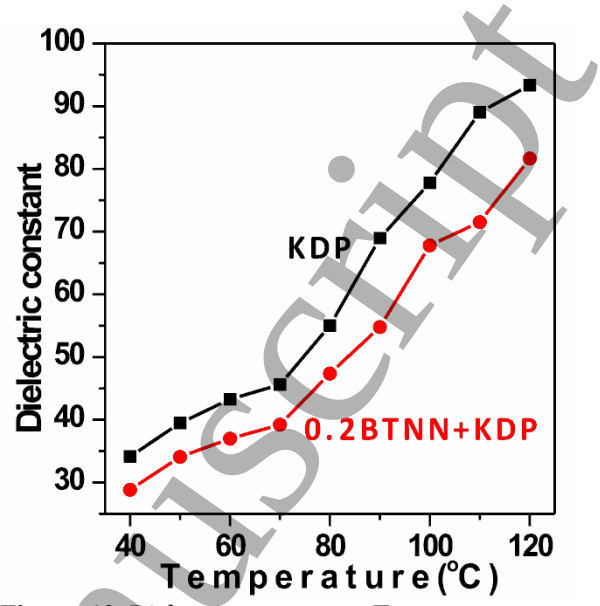

Figure 10 Dielectric constant vs. Temperature

The nonlinear refractive index (n_2) was calculated using the relation [25],

$$n_2 = \frac{\Delta\phi}{KI_0L_{eff}} \quad (2)$$

Where, K = 2π/ λ (λ is the wavelength of the incident laser beam), I_0 is the intensity of the laser beam at the focus, L_{eff} = [1-exp (-αL)]/α, is the effective thickness of the sample depending on linear absorption coefficient and L thickness of the sample.

Table 3 Optical resolution of z-scan setup

Laser beam wavelength (λ)	632.8nm
Lens focal length (f)	30 mm
Optical path distance (z)	85cm
Beam waist radius (w_a)	3.3 mm
Aperture radius (r_a)	2 mm
Sample thickness (L)	0.5 mm
Intensity at focus (I_0)	26.50MW/m^2

The Response of the crystal transmittance with the variation of crystal position along the direction of the laser beam (close aperture curve) is shown in figure 8. It reveals that BTNN doped KDP single crystal shows promising nonlinear refraction with a transmittance phase shift of valley to peak indicates that the sign of nonlinear refraction (n_2=1.51 x 10^{-9} cm^2/W) positive revealing the crystal have self-focusing tendency [26]. The doped KDP crystals with impressive positive nonlinear refraction are exclusively suitable for optical limiting and optical switching devices [27].The nonlinear absorption value was determined by the transmittance spectrum depicted in figure 9, which reveals that the positive nonlinear absorption in BTNN doped KDP crystal. The nonlinear absorption coefficient (β) of both doped KDP is evaluated according to above equation shown below,

$$\beta = \frac{2\sqrt{2}\Delta T}{I_0 L_{eff}} \quad (3)$$

Where, ΔT is the one valley value at the open aperture Z-scan curve and is depicted from figure 9. The value effective value of nonlinear absorption is found to be 5.57 x 10^{-6} cm/W. The real and imaginary parts of nonlinear susceptibility are calculated using the relations

$$\mathrm{Re}\,\chi^{(3)}(esu) = 10^{-4}(\varepsilon_0 C^2 n_0^{\,2} n_2)/\pi \quad (4)$$

$$\mathrm{Im}\,\chi^{(3)}(esu) = 10^{-2}(\varepsilon_0 C^2 n_0^{\,2} \lambda\beta)/4\pi^2 \quad (5)$$

Where ε_0 is the vacuum permittivity, c is the velocity of light and n_0 is the linear refractive index of the sample (n_0 =1.45). The third order nonlinear susceptibility of the 0.2 mole% BTNN doped KDP crystal is calculated using the formula

$$\chi^3(\mathrm{esu}) = \sqrt{(\mathrm{Re}\,\chi^3)^2 + (\mathrm{Im}\,\chi^3)^2} \quad (6)$$

The calculated value of the third order nonlinear susceptibility is 1.77 x 10^{-5} esu, signifies that grown crystal has notably greater value concludes that doped crystal has high polarizing nature than pure KDP. The decisive third order NLO refractive index, susceptibility and absorption coefficient for the doped crystal are summarized in Table 4. The values of refractive index, absorption coefficient and nonlinear susceptibility of the BTNN doped KDP crystal have wide applications in optical limiting and power switching devices [23, 28].

Table 4 Nonlinear optical parameters.

Crystal sample	n_2 (esu)	χ^3(esu)	β (cm/W)	Reference no.
KDP	2.34 x 10^{-13}	3.72x10-14		8
1 mol% FA + KDP	-1.14x 10^{-5}	3.81x10^{-7}	1.16x10^{-7}	8
1 mol% OA + KDP	2.25 x 10^{-5}	1.90x10^{-7}	1.14x10^{-7}	8
1 mol% MA + KDP	7.92x10^{-5}	2.13x10^{-7}	8.99x10^{-8}	8
1 wt% CA + KDP	-6.14x 10^{-16}	7.39x 10^{-4}	2.4x 10^{-4}	29
0.2 mol% BTNN + KDP	1.51 x 10^{-9}	1.77 x 10^{-5}	5.57 x 10^{-6}	Present study

3.3.4 Laser Damage Threshold Studies

The materials having a higher magnitude of laser damage threshold plays a vital role in the field of nonlinear optics and have wide optoelectronic device applications [30]. The laser damage threshold index depends on the materialistic properties like specific heat, thermal conductivity, optical absorption etc. and properties of laser source used for testing [31]. A pulsed Q-switched Nd:YAG laser incident with wavelength 1064 nm having laser beam diameter 1mm with repetition pulse rate of 10ns with operating in transverse TM00 mode. The polished surface of the crystal having thickness 5 mm is mounted on crystal holder and placed at the focal point of the lens. By increasing the power of incident laser radiation, the damaged spot on the crystal was clearly observed and at that radiation input laser energy density was recorded by the power meter. The Carl Zeiss optical microscope with a 50X magnification was used to measure the damaged spot on the crystal. The laser damage threshold of the grown crystal

is calculated by using relation I = E/τA where E is the input laser energy (mJ), τ is pulse width (ns) and A is the damaged circular area of the laser spot. The calculated value of laser damage threshold of BTNN doped KDP is found to be 11.72GW/cm^2 which is greater than that of KDP (0.20GW/cm^2) and urea (1.5 GW/cm^2). From this analysis, it is concluded that the BTNN doped KDP crystal is prominent material in the laser and optoelectronic applications [30].

3.4 Dielectric studies

The temperature dependent dielectric properties of pure and doped crystals were investigated at the frequency of 100 KHz using the Agilent 4284-A LCR cube meter. The dielectric constant of pure and doped KDP crystals was measured and their response with temperature is shown in figure 10. It is observed that the dielectric constant of both pure and doped KDP crystal increases with increasing range of temperature and the dielectric constant values for doped KDP have lower values than pure KDP. The dielectric constant of material is mainly due to the dipolar, ionic, electronic and space charge polarizations which are effective at lower frequencies [6].The lower dielectric constant of doped KDP indicates the lower power consumption ability of crystal which has applications in designing microelectronics devices, various high-speed telecommunication devices [32]. Figure 11 shows the dependence of dielectric loss as a function of temperature. The graph depicts that dielectric loss increases with a rise in temperature. The lower value of dielectric loss suggests the superior optical quality with fewer defects of doped KDP crystal with lower electrically defects. Thus lower dielectrics of BTNN doped KDP crystal vitalize its suitability for fabrication of electro-optic and NLO devices [33].

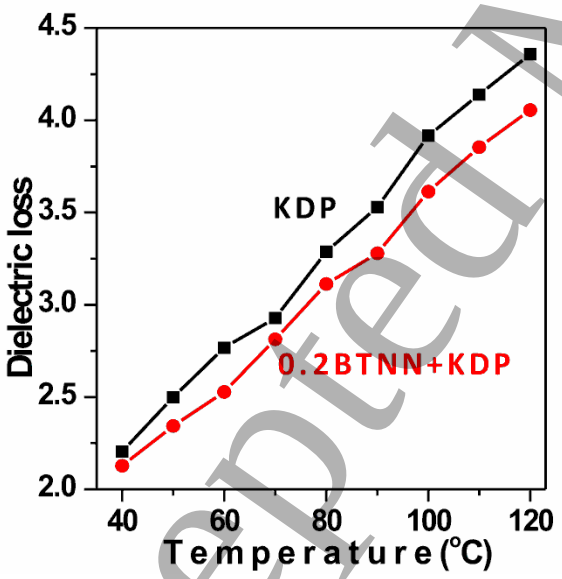

Figure 11 Dielectric loss vs. Temperature

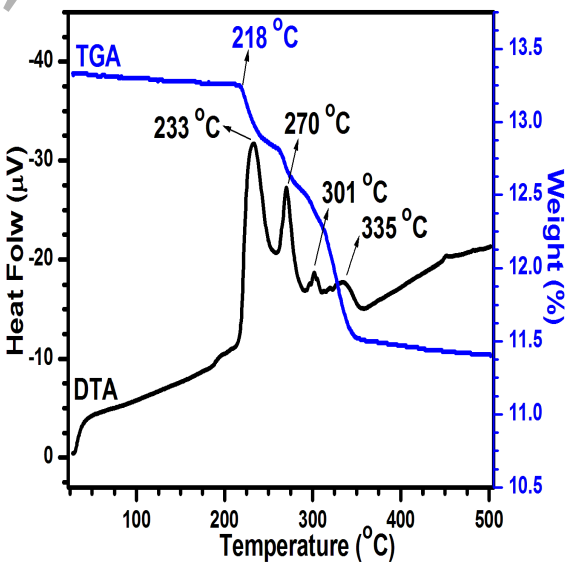

Figure 12 TGA/DTA Analysis

3.5 Thermal studies

The thermogravimetric and differential thermal analysis (TG/DTA) of BTNN doped KDP crystal has been recorded in a homogeneous nitrogen atmosphere in the range of 30 to 500^{0}C by employing the temperature increase at a rate of 10^{o}C/min. The thermogram recorded using the Shimadzu DTG-60H instrument is shown in figure 12. The sample weight used during the TGA/DTA process is 9.140 mg. The analysis of TG curve reveals no

decomposition of doped material up to 218°C confirming the absence of water or solvent inclusions in grown BTNN doped KDP crystal material [34]. The simultaneous weight loss of doped material has been observed in minor steps in the temperature range 218°C to 340°C. Further, the DTA curve shows that the decomposition endothermic peaks were consequently observed at 233°C, 270°C, 301°C and 335°C. The major and sharp endothermic peak in the DTA curve at 233°C confirms the melting point of grown crystal which is a vital parameter to subject the crystal for laser application. The higher the melting point of the material reveals good crystalline perfection and purity of the sample. The 0.2 mole% BTNN doped KDP crystal has higher thermal stability than the reported doped ADP and KDP materials [11, 13, 22]. The results of the TG-DTA analysis shows grown crystal have good thermal behavior and can be used NLO applications up to 233°C [35].

Table 5 Hardness parameters of BTNN doped KDP crystal

Load P (g)	H_V (Kg/mm^2)	C_{11} x 10^{14} (Pa)	σ_y (MPa)	K_c x10^4 (Kg/m$^{3/2}$)	B_i(m$^{-1/2}$)
25	8.484	42.18	5.64	0.4	1894
50	14.35	105.80	9.54	0.8	1602
100	20	189.14	13.3	1.7	1116

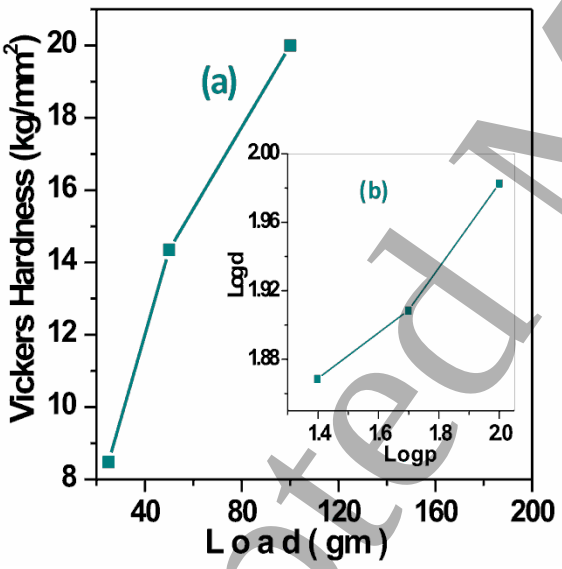

Figure 13 (a) Vickers hardness number vs. Load
(b) Log p vs. Log d

3.6 Mechanical studies

The Vickers hardness testing of 0.2mole% BTNN doped KDP crystal was carried out using Shimadzu, HMV-2T microhardness tester. For each load P, an average of two impressions was recorded and the average of diagonal lengths (d in mm) of the indentation mark after unloading was measured using a calibrated micrometer attached to the eyepiece of the microscope. The mechanical strength of the pure KDP and BTNN doped KDP crystals were observed by applying loads of 25g, 50g and 100g for constant indentation time 5 Sec. The Vickers microhardness value was calculated using formula, $H_v = 1.8544\ (P/d^2)$ Kg/mm^{2,} where p is the applied load (g) and d

is the average diagonal length (mm) of the indentation mark [36]. The plot of Vicker's hardness (H_v) versus load (P) for doped KDP crystal is shown in figure 13(a). From the graph, the property material in which linear response of hardness number with the applied indentation loads is known as reverse indentation size effect (RISE) [37]. The Meyer's law gives an expression regarding load and size of indentation, $p=k_1 \times d^n$, where, k_1 is the material constant and n is work hardening index. The graph is plotted between logp and logd, as shown in figure 13(b), and n value is found to be 4.7 According to Onitsch criterion, the calculated n value suggests that the grown crystal belongs to soft material [20]. The elastic stiffness coefficient was calculated using Wooster's empirical relation as $C_{11} = H_v^{7/4}$ and are shown in Table 5. The yield strength (σ_y) of the grown crystal was calculated by using formula $\sigma_y = (0.1)^{n-2} H_v/3$ and is shown in Table 5. The resistance to fracture indicates the toughness of a material and the fracture toughness K_c determines how much fracture stress is applied under uniform loading and is given by a relation $K_c = P/\beta_0 l^{3/2}$ for $l \geq d/2$[38]. Where β_0 is the indenter constant, equal to 7 for the Vickers's diamond pyramid indenter and the crack length (l) is the average of two crack lengths for each indentation. The fracture toughness (K_c) is calculated for the doped material is 0.4 x 10^4 Kg $m^{-3/2}$, is 0.8 x 10^4 Kg $m^{-3/2}$ and is 1.7 x 10^4 Kg $m^{-3/2}$ at 25, 50 and 100 g respectively. Brittleness is the property of a material which affects the mechanical behavior of a material, and is expressed in terms of the brittleness index (B_i) as $B_i = H_v / K_c$ [38]. The brittleness index (B_i) is calculated for the doped material is 1894 $m^{-1/2}$, 1602 $m^{-1/2}$ and 1116$m^{-1/2}$ at 25, 50 and 100 g respectively. The increase in hardness parameters might serve significant which offer less cracking/breaking/wastage of crystal material during crystal polishing and processing for device fabrication [39-40].

4. Conclusions

The 0.2 mole% BTNN doped KDP crystal has been grown by slow evaporation method at room temperature. The Single crystal XRD study confirms the tetragonal I structure with space group I(-4)2d. The enhancement in second order NLO response was confirmed by Kurtz-Perry powder test. The SHG efficiency of doped KDP crystal was found to be 1.98 times higher than that of KDP crystal. The UV- visible study shows that the high transparency of doped crystal in the entire visible region than pure KDP crystal and suitable band gap value, have applications in NLO and optical devices. The third order nonlinear susceptibility of grown crystal was found to be 1.77 x 10^{-5} esu, and studies reveal the strong self-focusing nature. The grown crystal has superior laser damage threshold (11.72 GW/cm^2) at 1064 nm wavelength of Nd:YAG pulsed laser. The microhardness studies confirmed that the doped KDP crystal exhibit improved mechanical behavior than pure KDP crystal and belongs to a soft material category and suggests the suitability of material in device fabrication. The thermal study reveals that the doped material is used for NLO applications up to 233^{o}C. The dielectric constant and dielectric loss of doped KDP crystals are lower than pure KDP crystal hence doped crystal has applicable in electro-optic modulation and NLO devices. The BTNN doped KDP crystal with improved crystalline perfection, influential optical, applicative mechanical, optimum thermal stability and enhanced electrical properties are a suitable material for NLO and photonic devices fabrications.

Acknowledgement

The authors are also thankful to Dr. Babu Varghese, IIT Madras for single crystal XRD analysis and also thankful to Rev. Dr. S. Johnbritto, Director, ACIC - Instrumentation Center, St. Joseph's College, Trichy, India for mechanical studies. One of the authors is thankful for UGC (UGC/41-591/2012/SR), New Delhi for financial assistance.

References

[1] R. Uthrakumar, C. Vesta, C. Justin Raj, S. Krishnan, S. Jerome Das 2010 *Curr. Appl. Phys.* **10** 548–552.

[2] S. S. Hussaini, N.R. Dhumane, V.G. Dongre, M.D. Shirsat 2009 *Mater. Sci.-Poland* **27** 365-372.

[3] Ferdousi Akhtar, Jiban Podder 2011 J. *Cryst. Process Technol.* **1** 55-62.

[4] P. Kumaresan, S. Moorthy Babu 2007 J. *Optoelectron. Adv. Mater.* **9** 1299-1305.

[5] K.D. Parikh, B.B. Parekh, D.J. Dave, M.J. Joshi 2013 *J. Cryst. Process Technol.* **3** 92-96.

[6] Mohd Anis, G.G. Muley, M.D. Shirsat, S.S. Hussaini 2015 *Cryst. Res. Technol.* **50** 372-378.

[7] Mohd Anis, M.D. Shirsat, Gajanan Muley, S.S. Hussaini 2014 *Phys. B* **449** 61-66.

[8] Mohd Anis, G.G. Muley, A. Hakeem, M.D. Shirsat, S.S. Hussaini 2015 *Opt. Mater.* **46** 517-521.

[9] P. Kumaresan, S. Moorthy Babu, P.M. Anbarasan 2007 *J. optoelectro. Adv. Mater.* **9** 2774 – 2779.

[10] M. Ugine Prince, P. Sujatha Therese & S.Perumal 2015 *J. Engine. Res. Appl.* **5** 07-14.

[11] P. Rajesh, P. Ramasamy, C.K. Mahadevan 2014 *Mater. Resear. Bullet.* **49** 640–644.

[12] Y.B. Rasal, M. Anis, M.D. Shirsat, S.S. Hussaini, Growth, 2017 Growth, *Mater. Res. Innovat.* **21** 45-49.

[13] P. Kumaresan, S. Moorthy Babu, P. M. Anbarasan 2007 *J. optoelectron. Adv. Mater.* **9** 2787 – 2791.

[14] V. Revathi and V. Rajendran 2013 *Der Pharma Chemica*, **5** 105-111.

[15] Norman B. Colthup, L.H. Daly, S.E. Wiberley 1990 *Infrared Spectroscopy*, American Cyanamid Company San Diego California. Toronto Print Book ISBN: 9780121825546, eBook ISBN: 9780080917405.

[16] Foil A. Miller & Charles H. Wilkins, 1952 *Infrared Spectra and Characteristics Frequencies of Inorganic Ions* **24** Mellon Institute, Pittsburgh 13.

[17] S.K. Kurtz, T.T. Perry 1968 J. Appl. Phys. **39** 3798-3813.

[18] G. Ramasamy, G. Bhagwannarayanan, Subbiah Meeakshisundaram 2014 *Indian J. pure appl. physics* **52** 255-261.

[19] R.N. Shaikh, M.D.Shirsat, P.M.Koinkar, S.S.Hussaini 2015 *Opt. Laser Technol.* **69** 8–12.

[20] P. Geetha, S. Krishnan, R.K. Natarajan, V. Chithambaram 2015 *Curr. Appl. Phys.* **15** 201-207.

[21] T. C. Sabari Girisun & S. Dhanuskodi 2009 *Cryst. Res. Technol.* **44** 1297 – 1302.

[22] R.N. Shaikh, Mohd. Anis, M.D. Shirsat, S.S. Hussaini 2015 *Spectrochim. Acta A* **136** 1243–1248.

[23] R.N. Shaikh, Mohd. Anis, M.D. Shirsat, S.S. Hussaini 2014 IOSR *J. Appl. Phys.* **6** 42-46.

[24] Mansoor Sheik-Bahae, Ali A. Said, Tai-Hue Wei, David J. Hagan, E.W. Van Stryland 1990 *J. Quant. Electron.* **26** 760–769.

[25] T. Sivanesan, V. Natarajan, S. Pandi 2010 *J. Sci. Technol.* **3** 653-655.

[26] V. Natarajan, T. Sivanesan, S. Pandi 2010 *J. Sci. Technol.*, **3** 656-658.

[27] K. Senthil, S. Kalainathan, F. Hamada, M. Yamada, P.G. Aravindan 2015 *Opt. Matei.* doi.org/10.1016/j.optmat.2015.05.029.

[28] T. Kanagasekaran, P. Mythili, P. Srinivasan, Ahmad Y. Nooraldeen, P. K. Palanisamy & R. Gopalakrishnan 2008 *Cryst. Growth Desi.* **8** 72335-2339.

[29] Mohd Anis, D.A. Hakeem, G.G. Muley, 2016, *Results in Physics*, doi.org/10.1016/j.rinp.2016.09.001.

[30] K. Senthila, S. Kalainathana, Fumio Hamada, Yoshihiko Kondo 2015 *RSC Advan.* DOI: 10.1039/C5RA14186A

[31] A. Senthil, P. Ramasamy, 2014 *J. Cryst. Growth*, doi.org/10.1016/j.jcrysgro.2014.01.022.

[32] G. Shanmugam, K. Thirupugalmani, R. Rakhikrishna, J. Philip, S. Brahadeeswaran 2013 *J. Therm. Anal. Calorim.* Doi 10.1007/s10973-013-3156-6.

[33] Delci Zion, Shyamala Devarajan, Thayumanavan Arunachalam 2013 *J. Cryst. Processes Technol.* **3** 5-11.

[34] N. R. Dhumane, S. S. Hussaini, V. G. Dongre, P. P. Karmuse & M. D. Shirsat 2009 *Cryst. Res. Technol.* **44** 269 – 274.

[35] M. Nirosha, S. Kalainathan, S. Sarveswari, V. Vijayakumar, A. Srikanth 2015 *Spectrochem. Acta A,* **137** 23–28.

[36] M. Senthil Pandian, Urit CharoenIn, P. Ramasamy, Prapun Manyum, M. Lenin, N. Balamuru. 2009 *J. of Cryst. Growth* doi: 10.1016 /j.jcrysgro. 2009.10.060.

[37] Suresh Sagadevan, Shanmuga Sundaram 2014 *J. Mater. Engg.* **4** 70-74. Doi: 10.5923/j.ijme.20140402.04.

[38] M Lakshmipriya, D Rajan Babu, R Ezhil Vizhi 2015 *Mater. Sci. and Enginee.* **73** 012091 doi: 10.1088/1757-899X/73/1/012091.

[39] Mohd Anis, G.G. Muley *Opt. Laser Technol.* **90** (2017) 190-196.

[40] Mohd Anis, G.G. Muley *Phys. Scr*. **91** (2016) 85801-85808.